

Full Length Research Paper

# Application of solid-state NMR methods in Coke characterization

Awatef Al-Adwani\*, Andre' Hauser and Fatima A. Ali

Kuwait Institute for Scientific Research, P.O. Box 24 885, Safat 13 109, Kuwait

Accepted 17 March, 2014

**Catalyst deactivation is a problem of great and continuing concern in residue hydroprocessing operations. It is widely accepted that the deactivation of hydrotreating catalysts is to a great extent caused by coke deposition. Three used commercial catalysts were studied by solid-state  $^{13}\text{C}$  NMR to derive structural information on the coke.  $^{13}\text{C}$  NMR spectral editing (cross polarization technique in combination with the polarization inversion pulse sequence) was applied to distinguish on the one hand between quaternary and tertiary aromatic carbon and on the other hand between secondary and primary aliphatic carbon. Structural parameters, derived from those NMR measurements in combination with the aromaticity from single pulse excitation  $^{13}\text{C}$  NMR and the H/C ratio from elemental analysis, have been used to obtain structural information on coke.**

**Key words:** *Coke, solid-state  $^{13}\text{C}$  NMR spectral editing, coke structure elucidation.*

## INTRODUCTION

Since high resolution solid-state  $^{13}\text{C}$  NMR has become a routine technique, NMR is a common and powerful tool for structural characterization of coke deposits. Due to such techniques as high power proton decoupling, cross polarisation (CP) and magic angle spinning (MAS) different types of carbon atoms can be resolved and it is possible to determine the aromaticity of the deposited coke. Although, CP/MAS  $^{13}\text{C}$  NMR (Fyfe, 1984) is the most commonly used method in high resolution solid-state NMR studies of dilute nuclear spin systems there are a number of problems in view of quantification. CP/MAS  $^{13}\text{C}$  NMR experiments are not necessarily quantitative.

The  $^{13}\text{C}$  intensity not only depends on the number of carbon atoms in distinct structural groups but also on the efficiency of the CP process for each kind of carbon in these structural groups (Richardson and Haw, 1989). Usually, protonated carbon is overestimated compared to nonprotonated one and  $\text{CH}_2$  carbon is slightly suppressed compared to  $\text{CH}_3$  one (Rethwisch, et al., 1993). Therefore, more reliable results are obtained by the

single pulse excitation sequence (SPE) (Fonseca et al., 1996) rather than by the more sensitive and faster CP technique (Maroto-Valer, et al., 1996).

The proton gated decoupling technique, applied along with the SPE technique, reduces the nuclear Overhauser effect (NOE) factor to zero. Since paramagnetic impurities are usually incorporated in carbonaceous deposits a relaxation delay of 10s for quantitative SPE/MAS  $^{13}\text{C}$  NMR measurements is satisfactory to ensure the evolution of the carbon magnetization to its equilibrium value before the next pulse cycle starts (Munson and Haw, 1990).

Carbonaceous deposits like coke form a very complex highly condensed aromatic structure and it is desirable to derive from solid-state  $^{13}\text{C}$  NMR spectra more than only the ratio of aliphatic and aromatic carbon. The access to further average structural parameters like tertiary aromatic carbon ( $\text{C}_{\text{ar};\text{t}}$ : CH) and quaternary aromatic carbon ( $\text{C}_{\text{ar};\text{q}}$ : C) like alkyl substituted carbon ( $\text{C}_{\text{ar};\text{R}}$ ), carbon in bridge head position of condensed aromatic rings ( $\text{C}_{\text{ar};\text{b}}$ ) and carbon connected to heteroatoms like N, S, O ( $\text{C}_{\text{ar};\text{X}}$ ) is hampered by a severe overlapping of the  $^{13}\text{C}$  signals assigned to these structural building blocks with the resonances of tertiary aromatic carbon. To overcome that drawback, Wu and Zilm proposed in 1993

\*Corresponding authors: E-mail: [awadwani@safat.kisr.edu.kw](mailto:awadwani@safat.kisr.edu.kw)

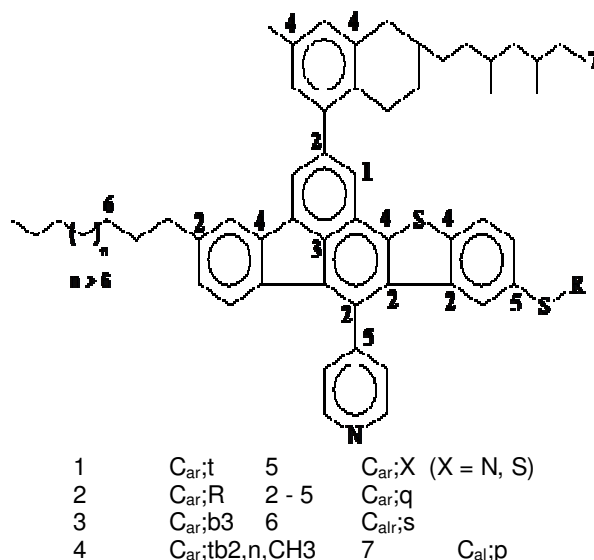


Figure 1: Hypothetical structure of deposited coke.

**Table 1:** Assignment of Carbon Resonances and their Chemical Shift Ranges in Solid-State MAS  $^{13}C$  NMR of Carbonaceous Deposits on Spent Catalysts

Abbreviation <sup>1)</sup>	Description	Chemical Shift Range <sup>2)</sup> in ppm
$I_{total}$	Entire NMR visible carbon	0 - 170
$C_{al}/I_{al}$	Aliphatic carbon	0 - 70
$C_{al};p/I_{al};p$	Primary, aliphatic carbon	0 - 28
$C_{al};s/I_{al};s$	Secondary, aliphatic carbon	28 - 70
$C_{ar}/I_{ar}$	Aromatic carbon	100 - 160
$C_{ar};t/I_{ar};t$	Tertiary, aromatic carbon	100 - 130
$C_{ar};q/I_{ar};q$ <sup>3)</sup>	Quaternary, aromatic carbon	128.5 - 160
$C_{ar};R/I_{ar};R$	Alkyl substituted aromatic carbon	138 - 150
$C_{ar};b3/I_{ar};b3$	Triplebridged aromatic carbon	123 - 126
$C_{ar};b2,n,CH_3/I_{ar};b2,n,CH_3$	Sum of doublebridged aromatic carbon, aromatic carbon attached to naphthenic rings or $CH_3$	128.5 - 138
$C_{ar};X/I_{ar};X$	Aromatic carbon attached to heteroatoms (N, S)	148 - 170
I <sub>ssb</sub>	Left edge spinning side band	170 - 225

<sup>1)</sup> C stands for % carbon causing a signal in the specified chemical shift region.

I stands for integral value in a.u. over the specified chemical shift region.

<sup>2)</sup> Storm et al., 1994, 1997; Altgeld et al., 1994.

<sup>3)</sup> except triplebridged aromatic carbon

a new pulse sequence which combines cross polarization with polarization inversion (CP/PI) at low or moderate MAS. Applying that pulse technique it is possible to distinguish between aromatic  $C_{ar};t$  and  $C_{ar};q$  as well as between aliphatic secondary ( $C_{al};s$ ;  $CH_2$ ) and primary carbon ( $C_{al};p$ ;  $CH_3$ ). A description of the method is given further down.

The structural characterization of carbonaceous deposits on spent catalysts is based on the fact that the

deposited hydrocarbons are formed of a limited number of building blocks which are shown in Figure.1.

These building blocks give rise to  $^{13}C$  NMR resonances within specific chemical shift ranges listed in Table 1. Integration over these chemical shift ranges leads to a quantification of the abundance of the building blocks in the coke.

In this study, SPE/MAS and CP/PI/MAS  $^{13}C$  NMR spectra of three commercial catalysts coked at operating

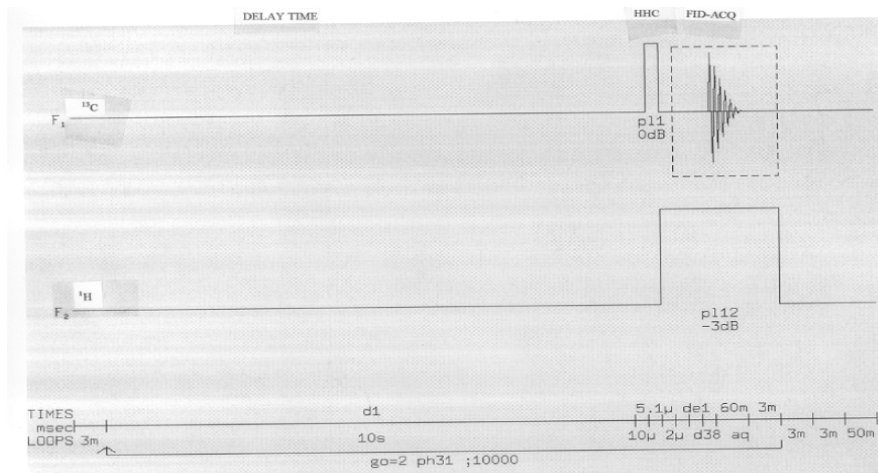


**Figure 2:** SPE/MAS  $^{13}\text{C}$  NMR Pulse programs.

**Table 2:** Operating Conditions for Coking of Catalysts A, B and C

Process Parameter	Condition
Temperature ( $^{\circ}\text{C}$ )	380
Pressure (bar)	120
LHSV ( $\text{h}^{-1}$ )	1.0
$\text{H}_2/\text{Oil}$ ratio (ml/ml)	680
Time-on-stream (h)	120

conditions as stated in Table 2 were measured and evaluated to obtain information on the coke structure.

## Experimental

### Materials

Three commercial hydroprocessing catalysts, in the form of extrudates, were acquired from a catalyst manufacturer. The three catalysts, which are labeled as catalysts A, B and C, are used as a catalyst system in commercial units. The major characteristics of the three catalysts (Marafi et al. 2003), including their composition, are presented in Table 3.

### Sample Preparation

The spent catalysts were Soxhlet extracted with toluene to remove carryovers from the feed and dried. Approximately 1g of the dry, spent catalyst sample was manually ground in a mortar until it was as homogeneous as possible. For proper spinning of the sample, the solid sample must be a dry, fine grain powder. The sample was filled either in a 7 mm (MAS: 4 kHz) or 4 mm rotor (MAS: 13 kHz).

## Solid-state NMR Spectroscopy

All NMR measurements were carried out on a BRUKER AVANCE 300 spectrometer (7.0463 T) equipped with a CP/MAS accessory and a fully automated pneumatic unit for sample spinning.

### SPE/MAS $^{13}\text{C}$ NMR

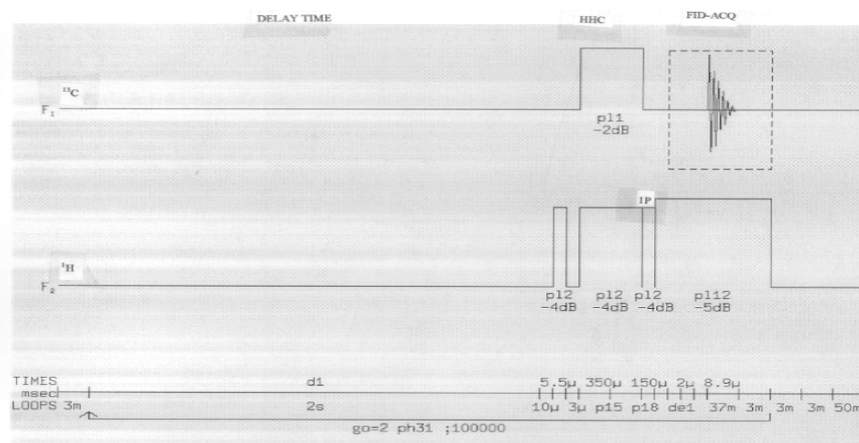
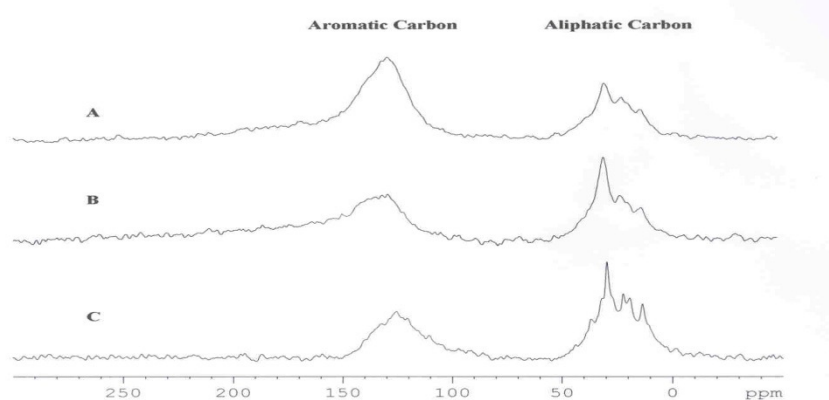
The spectra were obtained from ground samples using a 4mm multinuclear probe. MAS of 13 kHz was chosen to reduce the spinning side bands (SSB) to approximately 3 % of the center signal and to move them to the margins of the spectral range. The diagram of the pulse program is shown in Figure. 2. The pulse length of the  $^{13}\text{C}$  pulse was 3.6  $\mu\text{s}$  corresponding to  $90^{\circ}$  flip angle. The protons were inverse gated decoupled with maximum power (120 W). The recycling delay was 10 s.

### CP/PI/MAS $^{13}\text{C}$ NMR

The experiments were carried out under Hartman-Hahn conditions at a moderate MAS of 4kHz to minimize overlapping between the main signals (aliphatic and aromatic carbon) and the SSB. The diagram of the pulse

**Table 3:** Characteristics of Catalysts A, B, and C Used in the Present Study (Marafi et al., 2003)

Property	Catalyst		
	A	B	C
Bulk density (g/mL)	0.4-0.5	0.6-0.7	0.7-0.8
Surface area (m <sup>2</sup> /g)	150-200	200-250	170-200
Average pore diameter (Å <sup>o</sup> )	150-200	80-100	80-100
Type of active metals	Mo	Ni, Mo	Ni, Mo, P
Metal content (wt %)			
Mo	2-3	7-9	9-11
Ni		2-3	2-4
P			2-4
Metal capacity	high	medium	low

**Figure 3:** CP/PI/MAS <sup>13</sup>C NMR Pulse programs.**Figure 4:** Typical SPE/MAS <sup>13</sup>C NMR spectra of coke on Catalyst A, B and C

program is shown in Figure. 3. As contact time 350  $\mu$ s and as recycling delay 2 s were chosen. All spectra were measured with a sweep width of 55 kHz and the FID was sampled with 4 k data points.

## RESULTS AND DISCUSSION

Figure. 4 demonstrates typical SPE/MAS <sup>13</sup>C NMR spectra of coke on the used catalysts A, B and C. Peaks

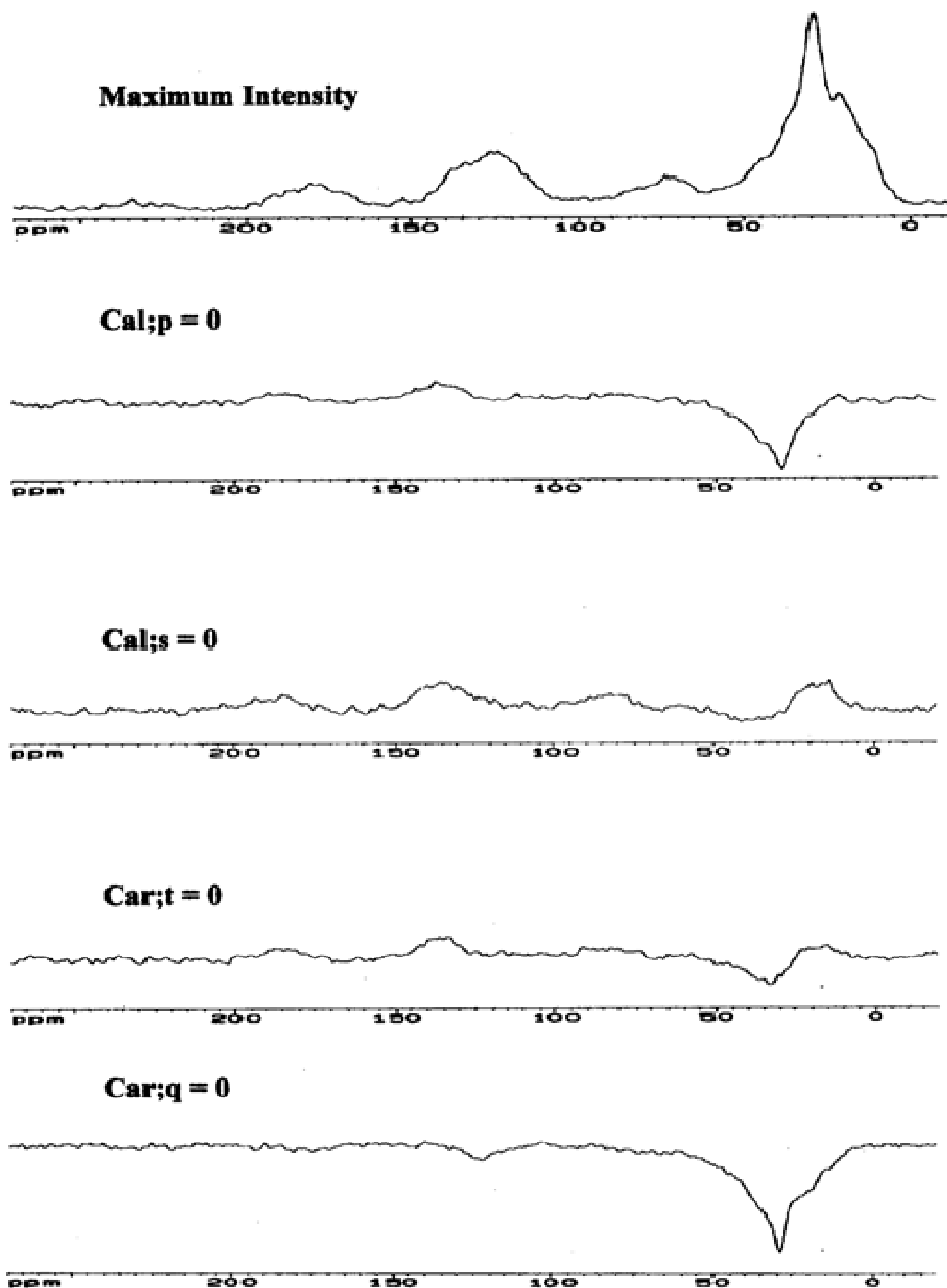


Figure 5: CP/PI/MAS  $^{13}\text{C}$  NMR spectra of spent catalyst A.

of aromatic and aliphatic carbon are denoted in the figure.

In order to obtain more structural information than merely the ratio of aromatic to aliphatic carbon in coke CP/PI/MAS  $^{13}\text{C}$  NMR was applied to the spent catalysts.

Figure 5 demonstrates that depending on the duration of the polarization inversion pulse the signal intensity of each type of carbon (primary;  $\text{C}_{\text{al};\text{p}}$ , secondary;  $\text{C}_{\text{al};\text{s}}$ , tertiary;  $\text{C}_{\text{ar};\text{t}}$ , quaternary;  $\text{C}_{\text{ar};\text{q}}$ ) in coke is nullified,

depending on the number of protons attached to it. Thus, as the secondary ( $^{13}\text{C}_{\text{al};\text{s}} = 0$  in Figure. 4) or tertiary carbon ( $^{13}\text{C}_{\text{ar};\text{t}} = 0$  in Figure. 4) is suppressed neither the remaining  $^{13}\text{C}_{\text{al};\text{p}}$  nor the  $^{13}\text{C}_{\text{ar};\text{q}}$  signal contain resonances of the  $^{13}\text{C}_{\text{al};\text{s}}$  or  $^{13}\text{C}_{\text{ar};\text{t}}$ .

Figure. 6 shows the intensity (initial intensity set to 100%) vs. polarization inversion pulse length plots for quaternary, tertiary, secondary and primary carbon. The signal intensities were measured at 140 ppm, 120 ppm,

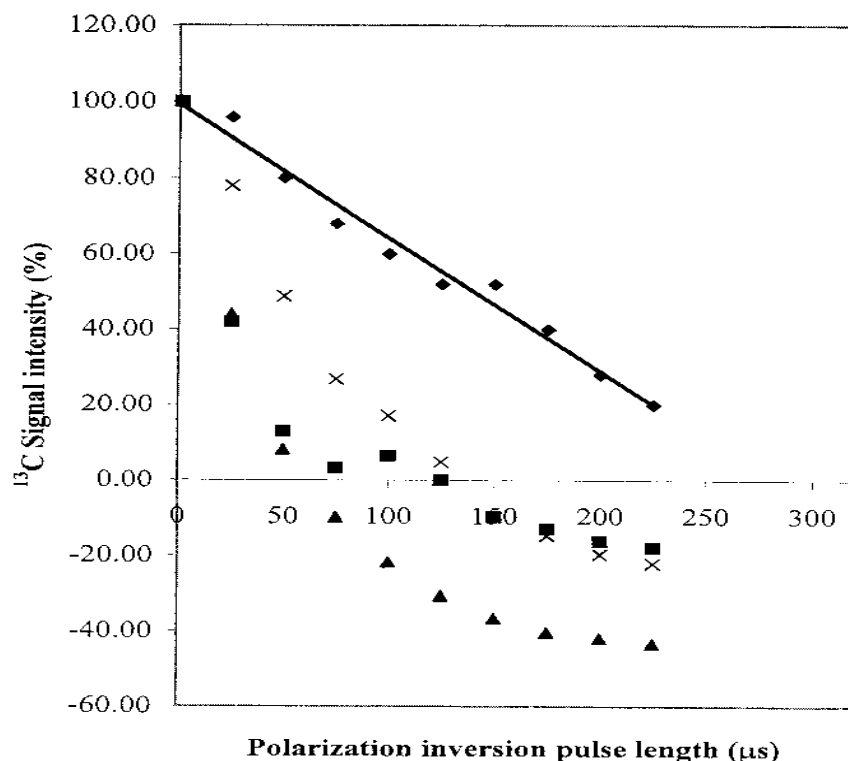


**Figure 6:**  $^{13}\text{C}$  Signal intensity vs. polarization inversion pulse length for  $^{13}\text{C}_{\text{ar};\text{q}}$  (◆),  $^{13}\text{C}_{\text{ar};\text{t}}$  (■),  $^{13}\text{C}_{\text{al};\text{s}}$  (▲) and  $^{13}\text{C}_{\text{al};\text{p}}$  (x) on used catalyst A measured at MAS = 4 kHz and Hartmann-Hahn conditions.

30 ppm and 14 ppm, respectively. The graphs demonstrate that the  $^{13}\text{C}_{\text{ar};\text{q}}$  intensity decreases linearly before the  $^{13}\text{C}_{\text{ar};\text{t}}$  intensity passes through zero. Thus, spectra measured at maximum positive intensity (max.) and at zero intensity (0) of  $\text{C}_{\text{ar};\text{t}}$  along with the aromaticity (fa) obtained from SPE/MAS  $^{13}\text{C}$  NMR can be used to calculate the fractions of  $\text{C}_{\text{ar};\text{t}}$ ,  $\text{C}_{\text{ar};\text{q}}$ ,  $\text{C}_{\text{ar};\text{R}}$  (alkyl substituted aromatic carbon),  $\text{C}_{\text{ar};\text{b3}}$  (triplebridged aromatic carbon), and  $\text{C}_{\text{ar};\text{b2},\text{n},\text{CH}_3}$  (sum of doublebridged aromatic carbon, aromatic carbon attached to naphthenic rings or  $\text{CH}_3$ ), using the following equations.

$$\text{C}_{\text{ar};\text{i}} = \left[ \frac{I_{\text{ar};\text{R}}}{I_{\text{ar}}}_{\text{max.}} \cdot \frac{I_{\text{ar};\text{i}}}{I_{\text{ar};\text{R}}}_0 \right] \cdot \text{fa} \cdot 100\% \quad (1)$$

$$\text{fa} = \frac{I_{\text{ar}} + 2 \cdot I_{\text{ssb}}}{I_{\text{total}}} \left[ \text{integrals from SPE } ^{13}\text{C NMR spectra} \right] \quad (2)$$

$$\text{C}_{\text{ar}} = \text{fa} \cdot 100\% \quad (3)$$

$$\text{C}_{\text{ar};\text{t}} = \left( \text{C}_{\text{ar}} - \text{C}_{\text{ar};\text{q}} \right)_{\text{max.}} \quad (4)$$

The integral values  $I_{\text{ar}}$ ,  $I_{\text{ssb}}$ ,  $I_{\text{total}}$ ,  $I_{\text{ar};\text{R}}$  and  $I_{\text{ar};\text{i}}$  are taken from the intervals listed in Table 1 in arbitrary unit. Depending on the structural building block the index i stands for q, b3, (b2,n,CH<sub>3</sub>), R, or X. Based on the above mentioned procedures five distinct carbon signals in the

aromatic region (100 – 160 ppm) and two in the aliphatic region (0 – 70 ppm) can be identified and quantified.

For aliphatic carbon the equations (5) and (6) have been applied. The factor (Fac.) is derived from the intensity vs. PIP length plot of  $\text{C}_{\text{al};\text{p}}$  and necessary to scale up  $(I_{\text{al};\text{p}})_0$  to its value at the PIP length of 0.1  $\mu\text{s}$ . Since the integral values  $(I_{\text{al};\text{p}})_0$  and  $(I_{\text{al}})_{\text{max}}$  are taken from different measurements they have to be comparable and not independently scaled.

$$\text{C}_{\text{as};\text{p}} = \text{Fac.} \cdot \frac{(I_{\text{al};\text{p}})_0}{(I_{\text{al}})_{\text{max}}} \cdot (1 - \text{fa}) \cdot 100\% \quad (5)$$

$$\text{C}_{\text{as};\text{s}} = \left( (I_{\text{al}} - I_{\text{al};\text{p}})_{\text{max}} \right) \cdot (1 - \text{fa}) \cdot 100\% \quad (6)$$

The indices (max.) and (0) in eqs. (5) and (6) indicate that the integral values were taken from spectra measured at maximum positive and at zero intensity of  $\text{C}_{\text{al};\text{s}}$ .

Combining data from solid-state  $^{13}\text{C}$  NMR and elemental analysis (Figure. 7) and by applying equations (1) to (6), the number of carbon atoms in different coke building blocks per 100 carbon atoms can be calculated. Based on these average, structural parameters, it is possible to construct hypothetical average substructures (Storm et al., 1994a) that match best these data.

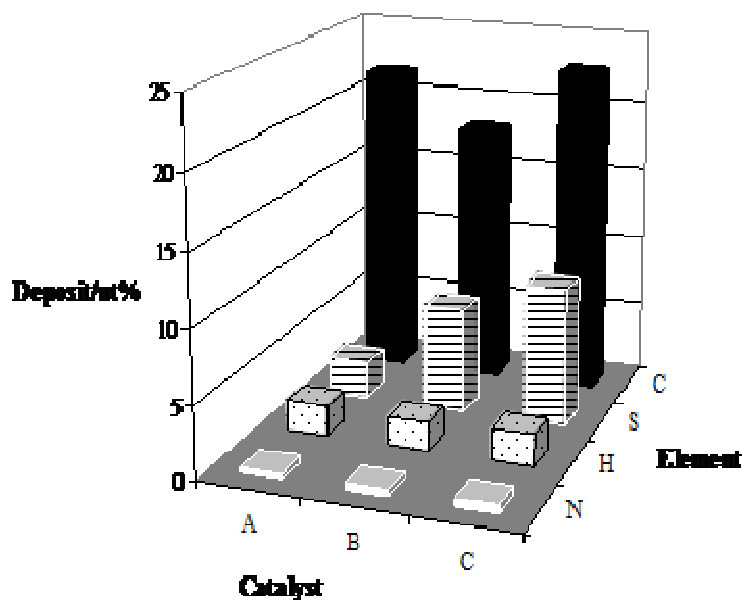


**Figure 7:** Elemental composition of coke on spent catalysts.

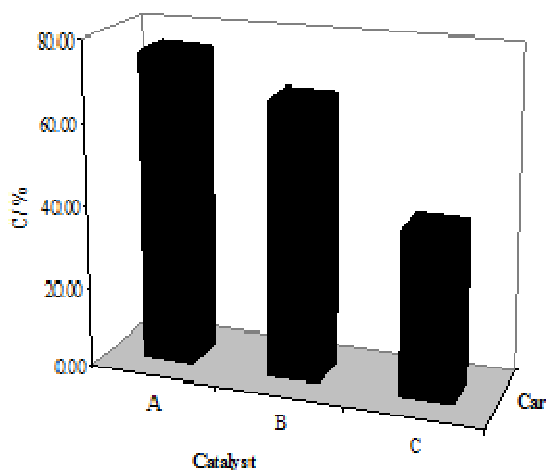


**Figure 8:** Fraction of aromatic carbon in coke on used catalysts.

The data presented in Figure. 8 show the fraction of aromatic carbon in coke formed on the catalysts A, B and C derived from SPE/MAS  $^{13}\text{C}$  NMR. Further structural features of the carbonaceous deposits are exhibited in Figures. 9 and 10. The structural features of the carbonaceous deposits, such as the aromaticity ( $f_a = [\text{Car} = \text{Car}/(\text{Car} + \text{Cal})]$ ), the degree of condensation ( $\gamma = [\text{Car}; b3 + \text{Car}; b2]/\text{Car}$ ) and substitution ( $\sigma = \text{Car}; \text{alk}/[\text{Car}; \text{alk} + \text{Car}; t]$ ), are comprised in Figure. 10. The examination of the data presented in Figures. 8 to 10

indicates that solid-state NMR is able to reflect differences in the coke structure. In case of initial coke on the catalyst system A, B, C, the coke structure depends on the type of catalyst. Catalyst A, which contains unpromoted Mo on  $\gamma$ -alumina, has a low hydrogenation activity yielding a coke, which is highly aromatic with a high content of quaternary carbon. The coke on the Ni-promoted catalyst B and the Ni-P-promoted catalyst C is less aromatic. The crack and dealkylation activity of catalyst C is fairly high, consequently, the aromatic rings

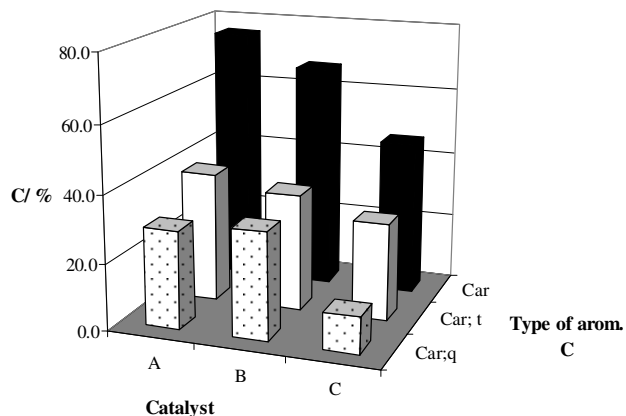


**Figure 9:** Type of aromatic carbon in coke on used catalysts.

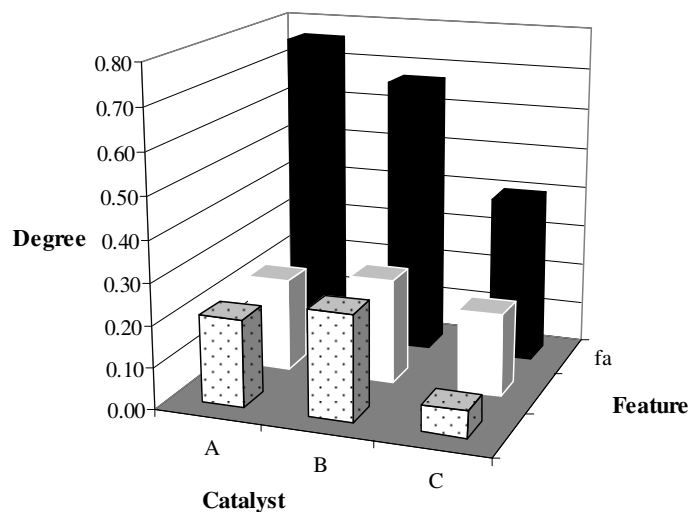


**Figure 10:** Structural features of coke on the used catalysts.

in the coke were cracked and alkyl side chains were cleaved, as indicated by the drop in the two parameters  $\gamma$  and  $\sigma$  (Figure. 10).

### Summary

Solid-state SPE/MAS and CP/PI/MAS  $^{13}\text{C}$  NMR combined with elemental analysis data provide an in-depth information on the carbon skeleton of carbonaceous deposit. Especially the polarization inversion (PI) technique, applied to a very complex hydrocarbon structure like coke, allows distinguishing on one hand between quaternary and tertiary aromatic carbon and on the other hand between secondary and primary aliphatic

carbon. Average structural parameters, such as aromaticity, degree of condensation and degree of alkyl-substitution can be derived from NMR measurements. The NMR technique proposed was applied to a catalyst system used in commercial refinery units. The results obtained indicate that during the initial phase of coking the coke structure depends to a great extent on the type of catalyst.

### CONCLUSION

Solid-state SPE/MAS and CP/PI/MAS  $^{13}\text{C}$  NMR combined with EA on used commercial HDM catalysts provide in-depth information on the carbon skeleton of

carbonaceous deposits. Especially the PI technique, applied to a very complex hydrocarbon structure like coke, allows distinguishing on one hand between quaternary and tertiary aromatic carbon and on the other hand between secondary and primary aliphatic carbon. Average structural parameters derived from those NMR measurements in combination with the H/C ratio of the coke leads to structural presentations per 100 carbon atoms, which can be repetitively joined to build-up the coke structure on the catalyst.

Three phases of initial coke formation have been observed. (i) Fast coke build-up on the catalyst (0–1 h/0–33% carbon on catalyst). The deposited coke consists of few condensed aromatic rings with shorter but heavily branched alkyl groups attached to them. (ii) Slow down of carbon deposition (1–12 h/33–39%). Accumulation of aromatic carbon and dealkylation/hydrogenation of aromatic rings take place. (iii) Reaching a steady state in carbon deposition (12–240 h/39–50%). Chemical transformation of the existing coke towards hydrogen rich aromatics and CH<sub>3</sub> deficient aliphatics continues. S as well as N, embedded in the deposit are slightly increasing. The hydrogenation activity of the HDM catalyst is still high and prevents the coke from getting hydrogen depleted merely the degree of alkyl-substitution has dropped significantly compared to the start of run. In the course of the ongoing refining process the carbon deposition converts into hydrogen deficient and highly condensed polyaromatic coke containing a high percentage of hetero-atoms.

## REFERENCES

- Altgelt KH, MM Boduszynki (1994) Composition and analysis of heavy Petroleum fractions. New York: Marcel Dekker, pp. 178-179.
- Fonseca A, P Zeuthen J, B Nagy (1996). <sup>13</sup>C NMR quantitative analysis of catalyst carbon deposition. *Fuel* 75, 1363-1376.
- Fyfe CA (1984). *Solid State NMR for Chemists*. C.F.C. Press, Guelph Canada.
- Marafi AS, Fucasi M, Al-Marri, A Stanislaus (2003). A comparative study on the effect of catalyst type on hydrotreating kinetics of Kuwaiti Atmospheric residue. *Energy&Fuel* 3: 661.
- Maroto-Valer MM, Andre'sen JM, Rocha DJ, Snape CE (1996). Quantitative solid-state <sup>13</sup>C n.m.r measurements on cokes, chars and coal tar pitch fractions. *Fuel* 75: 1721.
- Munson EJ, Haw JF (1990). Effect of paramagnetic Lanthanides on the study of carbonaceous deposits an Zeolite catalysts by carbon-13 solid-state nuclear magnetic resonance spectroscopy. *Anal. Chem.* 62: 2532.
- Rethwisch DG, Jacintha MA, Dybowski CR (1993). Quantification of <sup>13</sup>C in solids using CP MAS DD NMR spectroscopy. *Anal. Chem. Acta.* 283: 1033.
- Richardson BR, Haw JF (1989). Spin dynamics in the analysis of carbonaceous deposits on Zeolite catalysts by carbon-13 nuclear magnetic resonance with cross polarization and magic-angle spinning. *Anal. Chem.* 61: 1821.
- Storm DA, SJ Decanio, EY Sheu (1994). Sludgeformation during heavy oil conversion. In *Asphaltene Particles in Fossil Fuel Exploration, Recovery and Refining Processes*. Edited by M.K. Sharma and T.F. Yen. New York: Plenum Press, pp.81-90.
- Storm DA, JC Edwards, SJ DeCanio, EY Sheu (1994a). Molecular Representations of Ratawi and Alaska North Slope Asphaltenes Based on Liquid- and Solid-State NMR. **Energy and Fuels** 8: 561-566.
- Storm DA, SJ Decanio, JC Edwards, EY Sheu (1997). Sediment formation during heavy oil upgrading. *Petroleum Science and Technology* 15: 77-102.
- Wu X, KW Zilm (1993). Complete spectral editing in CPMAS NMR. *Journal Magnetic Resonance A* 102, 205-213.